J. Fluid Mech. (1983), *vol.* 127, *pp.* 519–537
Printed in Great Britain

Nonlinear oscillations of inviscid drops and bubbles

By JOHN A. TSAMOPOULOS AND ROBERT A. BROWN
Department of Chemical Engineering, Massachusetts Institute of Technology, Cambridge, MA 02139

(Received 29 March 1982)

Moderate-amplitude axisymmetric oscillations of incompressible inviscid drops and bubbles are studied using a Poincaré–Lindstedt expansion technique. The corrections to the drop shape and velocity potential caused by mode coupling at second order in amplitude are predicted for two-, three- and four-lobed motions. The frequency of oscillation is found to decrease with the square of the amplitude; this result compares well with experiments and numerical calculations for drops undergoing two-lobed oscillations.

1. Introduction

The free oscillations of drops and bubbles have been studied since the original reports by Savart (1833) and Plateau (1873) of the pulsating motions caused by the break-up of a liquid jet. The small-amplitude oscillations of an inviscid globe held together by interfacial tension were first analysed by Rayleigh (1879, see also Lamb 1932), who identified the fundamental modes of motion in terms of Legendre polynomials and calculated the corresponding frequencies. These linear results have been extended to include viscosity, first for a drop surrounded by a low-density gas (Reid 1960), and then for a drop in a viscous outer medium – by Miller & Scriven (1968) and more recently by Marston (1980) and Prosperetti (1980). Experiments (Marston & Apfel 1979, 1980; Trinh, Zwern & Wang 1982) performed on drops suspended in a neutrally buoyant and immiscible liquid have confirmed the oscillation frequencies of linear theory for small-amplitude deformations, but have shown a marked decrease in frequency with increasing amplitude (Trinh & Wang 1982). This decrease was anticipated by Rayleigh (1879), but has not been explained by either analysis or full numerical simulation of drop oscillations.

The only computer simulations for slightly viscous drops have been carried out by Foote (1973) and Alonso (1974). Both authors used the marker-and-cell finite-difference technique for solving time-dependent free-surface flows with viscosity, an extremely difficult numerical problem. The small number of calculations available in these works makes difficult the quantitative prediction of the sensitivity of the frequency and the evolution of the drop shape on the amplitude and mode of oscillation. The objective of the analysis presented here is to supply this insight.

We present asymptotic analyses for the moderate-amplitude axisymmetric oscillations of inviscid and incompressible liquid globes. As pointed out by Miller & Scriven (1968), the analysis of the motion of an interface separating two inviscid liquids leads to a discontinuity between the components of fluid velocity tangential to and on either side of the interface. The slip is a result of neglecting a viscous boundary layer that develops on both sides of the interface and removes the singularity in tangential velocity. We avoid the physically unacceptable results

associated with inviscid liquid/liquid systems by limiting our study to cases where one phase is either a vacuum or a tenuous gas, so that its hydrodynamical effects can be neglected. The two limits of liquid internal and external to the closed interface are denoted as drops and bubbles, respectively. In these single-fluid flows no boundary-layers develop as the viscosity of the liquid is taken to be zero.

The analysis is based on the method of Lindstedt and Poincaré (see Nayfeh & Mook 1979) for approximating the time-periodic solutions of nonlinear differential equations. Our approach to the problem of an oscillating drop parallels previous applications of this perturbation scheme to inviscid standing waves (Tadjbakhsh & Keller 1960; Concus 1962). The formulation of the problem and the perturbation solutions are given in §§2 and 3 respectively. The results are compared with the previous experiments and calculations in §4.

2. Formulation

2.1. *Drops*

We consider the time-periodic, irrotational and incompressible motion of an inviscid drop with volume $\bar{V} = \frac{4}{3}\pi R^3$, density ρ and interfacial tension σ. The surface of the drop during axisymmetric oscillations is described by $RF(\theta, t)$, where $F(\theta, t)$ is the dimensionless shape function of the drop and θ is the meridional angle in spherical coordinates. Scales based on the results of the linear theory are used to define the dimensional velocity potential $(\sigma R/\rho)^{\frac{1}{2}}\phi(r, \theta, t)$, pressure $(2\sigma/R)p(r, \theta, t)$, angular frequency $(\sigma/\rho R^3)^{\frac{1}{2}}\omega$, and time $(\rho R^3/\sigma)^{\frac{1}{2}}\omega^{-1}t$, each in terms of its dimensionless counterpart. The dimensionless radial coordinate is scaled with the static radius R of the drop. In terms of these variables the equations governing the inviscid time-periodic motion are

$$\nabla^2\phi = 0 \quad (0 \leqslant r \leqslant F(\theta, t), \quad 0 \leqslant \theta \leqslant \pi), \tag{1}$$

$$\partial\phi/\partial r = 0 \quad (r = 0, \quad 0 \leqslant \theta \leqslant \pi), \tag{2}$$

$$2p + \omega\frac{\partial\phi}{\partial t} + \frac{1}{2}\left[\left(\frac{\partial\phi}{\partial r}\right)^2 + \left(\frac{1}{r}\frac{\partial\phi}{\partial\theta}\right)^2\right] = G(t) \quad (0 \leqslant r \leqslant F(\theta, t), \quad 0 \leqslant \theta \leqslant \pi), \tag{3}$$

$$\frac{\partial\phi}{\partial r} = \omega\frac{\partial F}{\partial t} + \frac{1}{r^2}\frac{\partial\phi}{\partial\theta}\frac{\partial F}{\partial\theta} \quad (r = F(\theta, t)), \tag{4}$$

$$\Delta p_0 + 2p = \left\{-\frac{F_{\theta\theta}}{F} - \cot\theta\frac{F_\theta}{F}\left[1 + \left(\frac{F_\theta}{F}\right)^2\right] + 2 + 3\left(\frac{F_\theta}{F}\right)^2\right\}\left\{F\left[1 + \left(\frac{F_\theta}{F}\right)^2\right]^{\frac{3}{2}}\right\}^{-1} \quad (r = F(\theta, t)), \tag{5}$$

$$\nabla\phi(r, \theta, t + 2\pi) = \nabla\phi(r, \theta, t), \tag{6}$$

$$\int_0^\pi F^3(\theta, t)\sin\theta\, d\theta = 2, \tag{7}$$

$$\int_0^\pi\int_0^{2\pi} F(\theta, t)P_n(\theta)\sin\theta\cos t\, dt\, d\theta = \frac{2\pi\epsilon}{2n+1} \quad (n = 2, 3, \ldots), \tag{8}$$

$$\int_0^\pi\int_0^{2\pi} F(\theta, t)P_n(\theta)\sin\theta\sin t\, dt\, d\theta = 0 \quad (n = 2, 3, \ldots). \tag{9}$$

Equation (1) is the Laplace equation governing irrotational flow; (2) is the condition for a zero radial velocity at the centre of the drop; (3) is Bernoulli's equation for the

pressure everywhere in the drop; (4) is the kinematic condition relating the surface shape to the velocity field; (5) is the balance of dynamic and capillary pressure across the interface, where the right-hand side of this equation is the negative of the local mean curvature $2\mathscr{H}$ of the interface; (6) is the condition for the periodicity in time of the velocity field; (7) is the constraint for constant volume of the drop. The static pressure difference across the interface is Δp_0; the function $G(t)$ is introduced into (3) by integration. Equations (8) and (9) define the amplitude and phase of the oscillatory motion, respectively. If the shape function $F(\theta, t)$ is represented as a series of Legendre polynomials, the constraint (8) dictates that only the term proportional to $P_n(\theta)\cos t$ contributes to the amplitude ϵ. Equation (9) requires the shape function to be always orthogonal to $P_n(\theta)\sin t$ and hence sets the phase of the oscillation to be given by $\cos t$ alone.

2.2. *Bubbles*

The equation set governing the dynamics of bubbles is identical with (1)–(9) except that the velocity potential is defined external to the interface $F(\theta, t)$ and the boundary condition (2) is replaced by an appropriate far-field condition (11):

$$\nabla^2\phi = 0 \quad (F(\theta,t) \leqslant r \leqslant \infty, \quad 0 \leqslant \theta \leqslant \pi), \tag{10}$$

$$\frac{\partial\phi}{\partial r} = 0 \quad (r \to \infty, \quad 0 \leqslant \theta \leqslant \pi). \tag{11}$$

Also the sign on the pressure contribution in the Young–Laplace equation (5) is changed.

3. Perturbation solution

3.1. *Drops*

The solutions of the problem (1)–(9) are composed of the shape function $F(\theta, t)$, the velocity potential $\phi(r, \theta, t)$ and the frequency ω. We calculate these variables as the terms in expansions of the amplitude of the motion by the now classical Poincaré–Linstedt method (see Nayfeh & Mook 1979). This application is complicated by the dependence of the velocity potential $\phi(r, \theta, t)$ on the shape of the mathematical domain as given by the moving boundary $r = F(\theta, t)$. We account for changes in this boundary shape by combining the normal Poincaré–Linstedt expansion with the domain perturbation technique as detailed by Joseph (1973). To do this, the boundary shape is first immobilized as a sphere by introducing the change of coordinates $r \equiv \eta F(\theta, t)$. The expansions of the dependent variables in terms of ϵ are

$$\begin{pmatrix} f(\theta,t;\epsilon) \\ \phi(r,\theta,t;\epsilon) \\ \omega(\epsilon) \end{pmatrix} = \sum_{k=0}^{\infty} \frac{\epsilon^k}{k!} \begin{pmatrix} F^{(k)}(\theta,t) \\ \phi^{[k]}(\eta,\theta,t) \\ \omega^{(k)} \end{pmatrix}, \tag{12}$$

where

$$F^{(k)}(\theta,t) \equiv \frac{d^k F(\theta,t;0)}{d\epsilon^k}, \quad \omega^{(k)} \equiv \frac{d^k\omega(0)}{d\epsilon^k}, \quad \phi^{[k]}(\eta,\theta,t) \equiv \frac{d^k\phi(\eta,\theta,t;0)}{d\epsilon^k}. \tag{13}$$

The static spherical drop is recovered as the zeroth-order solution of the equation set, i.e. $F^{(0)}(\theta, t) = 1$ and $\phi^{(0)} = 0$, where the arbitrary reference potential inside the drop has been set to zero. Using the chain rule for differentiation, each term $\phi^{[k]}(\eta, \theta, t)$ in the expansion for the potential can be written as a sum of a contribution

evaluated on the spherical domain ($0 \leqslant \eta \leqslant 1, 0 \leqslant \theta \leqslant \pi$) and terms that account for the deformation of the domain at each order of ϵ. The first three relationships are

$$\phi^{[0]}(\eta, \theta, t; 0) \equiv \phi^{(0)}(\eta, \theta, t; 0), \tag{14a}$$

$$\phi^{[1]}(\eta, \theta, t; 0) \equiv \frac{\partial \phi}{\partial \epsilon}(\eta, \theta, t; 0) + F^{(1)}(\theta, t)\frac{\partial \phi}{\partial \eta}(\eta, \theta, t; 0)$$

$$\equiv \phi^{(1)}(\eta, \theta, t) + F^{(1)}(\theta, t)\frac{\partial \phi^{(0)}}{\partial \eta}, \tag{14b}$$

$$\phi^{[2]}(\eta, \theta, t; 0) = \phi^{(2)}(\eta, \theta, t) + F^{(2)}(\theta, t)\frac{\partial \phi^{(0)}}{\partial \eta} + F^{(1)2}\frac{\partial^2 \phi^{(0)}}{\partial \eta^2} + 2F^{(1)}(\theta, t)\frac{\partial \phi^{(1)}}{\partial \eta}, \tag{14c}$$

where $\phi^{(k)}(\eta, \theta, t) \equiv \partial^k \phi / \partial \epsilon^k$ are always defined in the spherical coordinate system ($0 \leqslant \eta \leqslant 1$, $0 \leqslant \theta \leqslant \pi$). As outlined by Joseph (1973), the equation sets governing the terms $\phi^{(k)}(\eta, \theta, t)$ account for changes in the domain shape only through corrections to the boundary conditions on the meniscus at each order of ϵ. These equation sets are presented below.

The expansion of the mean curvature in (5) is greatly facilitated if the corrections to the shape function are represented at each order as a series of Legendre polynomials:

$$F^{(k)}(\theta, t) = \sum_{m=0}^{\infty} F_m^{(k)}(\theta, t) = \sum_{m=0}^{\infty} \delta_m^{(k)}(t)\, P_m(\theta). \tag{15}$$

Then the mean curvature is expanded in terms of the amplitude as

$$-2\mathscr{H} = 2 + \epsilon \sum_{i=2}^{\infty} (i-1)(i+2) F_i^{(1)}(\theta, t) + \tfrac{1}{2}\epsilon^2 \Bigg\{ \sum_{j=0}^{\infty} (j-1)(j+2) F_j^{(2)}(\theta, t) - 4 \sum_{k=2}^{\infty} (k^2+k-1)(F_k^{(1)}(\theta, t))^2 \Bigg\} + O(\epsilon^3). \tag{16}$$

The equations governing the terms $(F^{(1)}, \phi^{(1)}, \omega^{(0)})$ are

$$\nabla^2 \phi^{(1)} = 0 \quad (0 \leqslant \eta \leqslant 1, \quad 0 \leqslant \theta \leqslant \pi), \tag{17}$$

$$\frac{\partial \phi^{(1)}}{\partial \eta} = 0 \quad (\eta = 0, \quad 0 \leqslant \theta \leqslant \pi), \tag{18}$$

$$\frac{\partial \phi^{(1)}}{\partial \eta} = \omega^{(0)} \frac{\partial F^{(1)}}{\partial t} \quad (\eta = 1), \tag{19}$$

$$\omega^{(0)} \frac{\partial \phi^{(1)}}{\partial t} + \sum_{n=2}^{\infty} (n-1)(n+2) F_n^{(1)}(\theta, t) = 0 \quad (\eta = 1), \tag{20}$$

$$\nabla \phi^{(1)}(\eta, \theta, t + 2\pi) = \nabla \phi^{(1)}(\eta, \theta, t), \tag{21}$$

$$\int_0^{\pi} F^{(1)}(\theta, t) \sin\theta \, d\theta = 0, \tag{22}$$

$$\int_0^{\pi} \int_0^{2\pi} F^{(1)} P_n(\theta) \sin\theta \cos t \, dt \, d\theta = \frac{2\pi}{2n+1} \quad (n = 2, 3, \ldots), \tag{23}$$

$$\int_0^{\pi} \int_0^{2\pi} F^{(1)} P_n(\theta) \sin\theta \sin t \, dt \, d\theta = 0 \quad (n = 2, 3, \ldots). \tag{24}$$

The pressure has been eliminated from (20) by substitution from the first-order form of Bernoulli's equation (3).

The equation set (17)–(24) has an infinite number of solutions, each of the form

$$F^{(1)}(\theta,t) \equiv F_n^{(1)}(\theta,t) = \cos tP_n(\theta),$$

$$\phi^{(1)}(\eta,\theta,t) \equiv \phi_n^{(1)}(\eta,\theta,t) = \frac{-(n-1)(n+2)}{\omega^{(0)}}\eta^n \sin tP_n(\theta), \tag{25}$$

$$\omega^{(0)} \equiv \omega_n^{(0)} = (n(n-1)(n+2))^{\frac{1}{2}} \quad (n = 2,3,\ldots),$$

which corresponds to the linear modes of oscillation analysed by Rayleigh (1879). The mode $n = 1$ describes a rigid translation of the drop and has been omitted so that the centre of mass of the drop is fixed with respect to the coordinate system.

The equations governing the terms $(F^{(2)}, \phi^{(2)}, \omega^{(1)})$ are

$$\nabla^2\phi^{(2)} = 0 \quad (0 \leqslant \eta \leqslant 1, \quad 0 \leqslant \theta \leqslant \pi), \tag{26}$$

$$\partial\phi^{(2)}/\partial\eta = 0 \quad (\eta = 0, \quad 0 \leqslant \theta \leqslant \pi), \tag{27}$$

$$\frac{\partial\phi^{(2)}}{\partial\eta} - \omega_n^{(0)}\frac{\partial F^{(2)}}{\partial t} = 2\omega^{(1)}\frac{\partial F_n^{(1)}}{\partial t} + 2\frac{\partial F_n^{(1)}}{\partial\theta}\frac{\partial\phi_n^{(1)}}{\partial\theta} - 2F_n^{(1)}\frac{\partial^2\phi_n^{(1)}}{\partial\eta^2} \quad (\eta = 1), \tag{28}$$

$$\omega_n^{(0)}\frac{\partial\phi^{(2)}}{\partial t} + \sum_{m=0}^{\infty}(m-1)(m+2)F_m^{(2)}$$
$$= -2\omega^{(1)}\frac{\partial\phi_n^{(1)}}{\partial t} - 2\omega^{(0)}F^{(1)}\frac{\partial^2\phi_n^{(1)}}{\partial\eta\,\partial t} - \left[\left(\frac{\partial\phi_n^{(1)}}{\partial\eta}\right)^2 + \left(\frac{1}{\eta}\frac{\partial\phi_n^{(1)}}{\partial\theta}\right)^2\right] + 4(n^2+n-1)F_n^{(1)2}$$
$$(\eta = 1) \tag{29}$$

$$\nabla\phi^{(2)}(\eta,\theta,t+2\pi) = \nabla\phi^{(2)}(\eta,\theta,t), \tag{30}$$

$$\int_0^{\pi}\{2F^{(1)2} + F^{(2)}\}\sin\theta\,d\theta = 0, \tag{31}$$

$$\int_0^{\pi}\int_0^{2\pi} F^{(2)}P_n(\theta)\sin\theta\cos t\,dt\,d\theta = 0, \tag{32}$$

$$\int_0^{\pi}\int_0^{2\pi} F^{(2)}P_n(\theta)\sin\theta\sin t\,dt\,d\theta = 0, \tag{33}$$

where the subscripts n denote the particular linear solution (25) for which the solutions of (26)–(33) hold.

The velocity potential $\phi^{(2)}$ is expanded in a Legendre series that satisfies (26) and (27),

$$\phi^{(2)}(\eta,\theta,t) = \sum_{m=0}^{\infty}\gamma_m(t)\,\eta^m P_m(\theta), \tag{34}$$

and the shape function $F^{(2)}$ is assumed to be given by (15). Equations (28) and (29) are reduced to a sequence of non-homogeneous second-order equations for the coefficients $\{\gamma_m(t)\}$ and the correction to the frequency $\omega^{(1)}$ by forming successively the integrals of (28) and (29) with each of the set $\{\sin\theta P_m(\theta)\}$. Applying the

orthogonality property of Legendre polynomials and eliminating the coefficients $\{\delta_m^{(2)}(t)\}$ between the two equations yields

$$\frac{d^2\gamma_m}{dt^2}+\frac{m(m-1)(m+2)}{\omega^{(0)2}}\gamma_m=\frac{(2m+1)(m-1)(m+2)}{2\omega^{(0)2}}\Big\{-4\omega^{(1)}\sin t\langle P_n,P_m\rangle$$
$$-\frac{(n-1)(n+2)}{\omega^{(0)}}\sin 2t\langle P_n'^2-(n-1)nP_n^2,P_m\rangle$$
$$+\frac{\omega^{(0)}}{(m-1)(m+2)}\sin 2t\Big[-2(n^3+3n^2-2)\langle P_n^2,P_m\rangle$$
$$-\frac{(n-1)^2(n+2)^2}{\omega^{(0)2}}\langle n^2P_n^2+P_n'^2,P_m\rangle\Big]\Big\}, \tag{35}$$

where the notation $\langle h(\theta),g(\theta)\rangle$ stands for the inner product

$$\langle h(\theta),g(\theta)\rangle\equiv\int_0^\pi h(\theta)g(\theta)\sin\theta\,d\theta. \tag{36}$$

The integrals in the non-homogeneous terms in the set (35) are expressed in terms of the well-known $3j$ and $6j$ symbols for spherical harmonics (Rotenberg *et al.* 1959) which extend the orthogonality properties of integrals of two Legendre polynomials to integrals involving products of three or four polynomials and their derivatives. Several formulae used in the reduction of equation (35) are listed in the appendix. Only a few of the integrals on the right-hand side of (35) are non-zero for each choice of the first-order solution (25), and these terms dictate the coupling of modes of oscillation that arise at second order. The algebra in this and subsequent manipulations is tedious, and the reduction of the formulas has been greatly expedited by the use of the symbolic manipulator MACSYMA (MACSYMA 1977; Pavelle, Rothstein & Fitch 1981) available on the M.I.T. computer system.

The non-trivial equations that result from (35) are as follows:

for $n=2$,

$$L_{22}(\gamma_2(t))=-2\omega^{(1)}\sin t-\frac{104}{7\omega^{(0)}}\sin 2t, \tag{37a}$$

$$L_{24}(\gamma_4(t))=\frac{324}{35\omega^{(0)}}\sin 2t; \tag{37b}$$

for $n=3$,

$$L_{32}(\gamma_2(t))=-\frac{32}{\omega^{(0)}}\sin 2t, \tag{38a}$$

$$L_{33}(\gamma_3(t))=-\tfrac{4}{3}\omega^{(1)}\sin t, \tag{38b}$$

$$L_{34}(\gamma_4(t))=-\frac{300}{11\omega^{(0)}}\sin 2t, \tag{38c}$$

$$L_{36}(\gamma_6(t))=\frac{3200}{77\omega^{(0)}}\sin 2t; \tag{38d}$$

for $n=4$,

$$L_{42}(\gamma_2(t))=\frac{-4150}{77\omega^{(0)}}\sin 2t, \tag{39a}$$

$$L_{44}(\gamma_4(t))=-\omega^{(1)}\sin t-\tfrac{53136}{1001}\sin 2t, \tag{39b}$$

$$L_{46}(\gamma_6(t))=\frac{-350}{11\omega^{(0)}}\sin 2t, \tag{39c}$$

$$L_{48}(\gamma_8(t))=\frac{124950}{143\omega^{(0)}}\sin 2t; \tag{39d}$$

where $$L_{nm}(\gamma_\mu(t)) \equiv \left[\frac{d^2(\ )}{dt^2} + \frac{m(m-1)(m+2)}{\omega_n^{(0)2}}\right]\gamma_m(t).$$

In forming these equation sets it has been assumed that the contribution of any purely homogeneous equation is zero. This is formally true only if m is constrained to satisfy

$$\frac{m(m-1)(m+2)}{\omega_n^{(0)2}} \neq (\text{integer})^2, \tag{40}$$

for $m \neq n$. Equation (40) excludes values of m for which the linear theory yields a time frequency that is an integral multiple of a fundamental frequency.

In each set the frequency correction $\omega^{(1)}$ is determined so that secular terms in the solution vanish, which leads to

$$\omega^{(1)} = 0 \quad (n = 2, 3, 4). \tag{41}$$

The solutions of (37)–(39) are then determined so that the constraints (31)–(33) are satisfied. The final forms for the corrections $(F^{(2)}, \phi^{(2)})$ are as follows:

for $n = 2$,

$$F^{(2)}(\theta, t) = -\tfrac{2}{5}\cos^2 t + \tfrac{11}{14}(1 - \tfrac{29}{33}\cos 2t)\,P_2(\theta) + \tfrac{18}{35}(1 + \tfrac{3}{5}\cos 2t)\,P_4(\theta), \tag{42}$$

$$\phi^{(2)}(\eta, \theta, t) = \frac{1}{\omega^{(0)}}[\tfrac{13}{5} + \tfrac{104}{21}P_2(\theta)\,\eta^2 + \tfrac{324}{175}P_4(\theta)\,\eta^4]\sin 2t; \tag{43}$$

for $n = 3$,

$$F^{(2)}(\theta, t) = -\tfrac{2}{7}\cos^2 t + \tfrac{22}{21}(1 - \tfrac{4}{11}\cos 2t)\,P_2(\theta) + \tfrac{101}{231}(1 - \tfrac{453}{202}\cos 2t)\,P_4(\theta) + \tfrac{130}{231}(1 + \tfrac{1}{13}\cos 2t)\,P_6(\theta), \tag{44}$$

$$\phi^{(2)}(\eta, \theta, t) = \frac{1}{\omega^{(0)}}[\tfrac{85}{14} + \tfrac{60}{7}P_2(\theta)\,\eta^2 + \tfrac{375}{22}P_4(\theta)\,\eta^4 + \tfrac{800}{77}P_6(\theta)\,\eta^6]\sin 2t; \tag{45}$$

for $n = 4$,

$$F^{(2)}(\theta, t) = -\tfrac{2}{9}\cos^2 t + \tfrac{3575}{2772}(1 - \tfrac{1097}{5005}\cos 2t)\,P_2(\theta) + \tfrac{927}{2002}(1 - \tfrac{301}{309}\cos 2t)\,P_4(\theta) + \tfrac{305}{792}(1 - \tfrac{263}{61}\cos 2t)\,P_6(\theta) + \tfrac{70}{117}(1 - \tfrac{2744}{9163}\cos 2t)\,P_8(\theta), \tag{46}$$

$$\phi^{(2)}(\eta, \theta, t) = \frac{1}{\omega^{(0)}}[\tfrac{21}{2} + \tfrac{7470}{539}P_2(\theta)\,\eta^2 + \tfrac{17712}{1001}P_4(\theta)\,\eta^4 + \tfrac{525}{11}P_6(\theta)\,\eta^6 + \tfrac{66150}{2431}P_8(\theta)\,\eta^8]\sin 2t. \tag{47}$$

The corrections to the velocity potential in the physical coordinate system (r, θ) are reconstructed by substituting the expressions for $\phi^{(1)}(\eta, \theta, t)$ and $\phi^{(2)}(\eta, \theta, t)$ into (12) and using the definition of the coordinate $\eta = r/F(\theta, t; \epsilon)$ to order ϵ^2.

The analysis is extended to third order in order to calculate the first non-zero correction to the frequency $\omega^{(2)}$. The corrections to the velocity potential and shape function $(\phi^{(3)}, F^{(3)})$ are written as expansions analogous to (34) and (15), and the kinematic and Young–Laplace equations are reduced to a sequence of decoupled second-order equations in time by the same procedure used to calculate the sets (37)–(39). The correction $\omega^{(2)}$ is determined so that the solutions to these equations contain no secular terms. We omit the details of this derivation, which are available in Tsamopoulos (1983) and list only the frequency corrections:

for $n = 2$,

$$\omega^{(2)} = -\tfrac{37559}{29400}\omega^{(0)} \approx -1{\cdot}27752\,\omega^{(0)}; \tag{48}$$

for $n = 3$, $$\omega^{(2)} = -\tfrac{4142179}{1981980}\omega^{(0)} \approx -2{\cdot}08992\omega^{(0)}; \tag{49}$$

for $n = 4$, $$\omega^{(2)} = -\tfrac{1889926349 13}{648655367 36}\omega^{(0)} \approx -2{\cdot}91361\omega^{(0)}. \tag{50}$$

Since the corrections $\omega^{(3)}$ will be identically zero, the terms (48–50) give predictions for the frequency that are valid up to fourth order in the amplitude.

The kinetic $\mathscr{K}$ and surface $\mathscr{P}$ energies of the drop are given by the expressions

$$\mathscr{K} \equiv \frac{1}{2}\int_V \nabla\phi \,.\, \nabla\phi \, dV, \quad \mathscr{P} \equiv \int_0^\pi (F^2 + F_\theta^2)^{\frac{1}{2}} F \sin\theta \, d\theta, \tag{51}$$

where V is the volume of the drop. These quantities are approximated as follows:

for $n = 2$, $$\mathscr{K} = \tfrac{4}{5}\epsilon^2 \sin^2 t + O(\epsilon^3), \quad \mathscr{P} = 2 + \epsilon^2 \tfrac{4}{5}\cos^2 t + O(\epsilon^3); \tag{52}$$

for $n = 3$, $$\mathscr{K} = \epsilon^2 \tfrac{10}{7} \sin^2 t + O(\epsilon^3), \quad \mathscr{P} = 2 + \epsilon^2 \tfrac{10}{7} \cos^2 t + O(\epsilon^3); \tag{53}$$

for $n = 4$, $$\mathscr{K} = \epsilon^2 2 \sin^2 t + O(\epsilon^3), \quad \mathscr{P} = 2 + \epsilon^2 2 \cos^2 t + O(\epsilon^3). \tag{54}$$

The lowest-order terms in both the kinetic and potential energies are due to ϵ-order corrections in the shape and velocity potential respectively, and thus do not represent the finite-amplitude behaviour of the oscillations.

3.2. *Bubbles*

The procedure for calculating the first- and second-order corrections to the frequency, shape and velocity potential for a bubble follows directly from that outlined in §3.1. The results are given here in the form of the series (12). The solutions to the first-order problem are

$$F^{(1)}(\theta, t) \equiv F_n^{(1)}(\theta, t) = P_n(\theta)\cos t, \tag{55a}$$

$$\phi^{(1)}(\eta, \theta, t) \equiv \phi_n^{(1)}(\eta, \theta, t) = \frac{(n-1)(n+2)}{\omega^{(0)}\eta^{n+1}} P_n(\theta)\sin t, \tag{55b}$$

$$\omega^{(0)} \equiv \omega_n^{(0)} = ((n^2-1)(n+2))^{\frac{1}{2}}. \tag{55c}$$

The second-order corrections $(F^{(2)}, \phi^{(2)}, \omega^{(1)})$ are as follows:

for $n = 2$,

$$F^{(2)}(\theta, t) = -\tfrac{2}{5}\cos^2 t + \tfrac{3}{7}(1 - \tfrac{7}{9}\cos 2t) P_2(\theta) + \tfrac{4}{105}(1 + \tfrac{228}{7}\cos 2t) P_4(\theta), \tag{56a}$$

$$\phi^{(2)}(\eta, \theta, t) = [-\tfrac{7}{5} + \tfrac{16}{21} P_2(\theta)\eta^{-3} + \tfrac{3072}{245} P_4(\theta)\eta^{-5}]\frac{\sin 2t}{\omega^{(0)}}, \tag{56b}$$

$$\omega^{(1)} = 0; \tag{56c}$$

for $n = 3$,

$$F^{(2)}(\theta, t) = -\tfrac{2}{7}\cos^2 t + \tfrac{53}{84}(1 - \tfrac{289}{1961}\cos 2t) P_2(\theta) + \tfrac{9}{154}(1 - 9\cos 2t) P_4(\theta) - \tfrac{185}{1848}(1 - \tfrac{1571}{111}\cos 2t) P_6(\theta), \tag{57a}$$

$$\phi^{(2)}(\eta, \theta, t) = [-\tfrac{55}{14} + \tfrac{500}{111} P_2(\theta)\eta^{-3} + \tfrac{2150}{63} P_6(\theta)\eta^{-7}]\frac{\sin 2t}{\omega^{(0)}}, \tag{57b}$$

$$\omega^{(1)} = 0, \tag{57c}$$

for $n = 4$,

$$F^{(2)}(\theta, t) = -\tfrac{2}{9}\cos^2 t + \tfrac{590}{693}(1 - \tfrac{71}{1711}\cos 2t) P_2(\theta) + \tfrac{9}{91}(1 - \tfrac{29}{33}\cos 2t) P_4(\theta) - \tfrac{2}{45}(1 + \tfrac{281}{11}\cos 2t) P_6(\theta) - \tfrac{1253}{6435}(1 - \tfrac{1351}{179}\cos 2t) P_8(\theta), \tag{58a}$$

$$\phi^{(2)}(\eta,\theta,t) = [-\tfrac{15}{2} + \tfrac{20400}{2233} P_2(\theta)\eta^{-3} + \tfrac{8532}{1001} P_4(\theta)\eta^{-5} - \tfrac{144}{11} P_6(\theta)\eta^{-7} + \tfrac{9212}{143} P_8(\theta)\eta^{-9}]\frac{\sin 2t}{\omega^{(0)}}, \quad (58b)$$

$$\omega^{(1)} = 0. \quad (58c)$$

The first non-zero corrections to the oscillation frequency appear at second order in amplitude and are as follows:

for $n = 2$, $$\omega^{(2)} = -\tfrac{44893}{30870}\omega^{(0)} \approx -1{\cdot}45426\omega^{(0)}; \quad (59)$$

for $n = 3$, $$\omega^{(2)} = -\tfrac{355251121}{159999840}\omega^{(0)} \approx -2{\cdot}22032\omega^{(0)}; \quad (60)$$

for $n = 4$, $$\omega^{(2)} = -\tfrac{143143247 79}{4939864930}\omega^{(0)} \approx -2{\cdot}89772\omega^{(0)}. \quad (61)$$

4. Results and comparisons

Representative shapes of drops and bubbles through a half-period of oscillation are shown on figures 1 and 2 for the lowest three fundamental modes of deformation, $n = 2, 3, 4$. In both figures, the continuous curves represent the shapes predicted by the first-order results and the dashed curves are the shapes corrected to second order in amplitude. In each case, the amplitude has been set to $\epsilon = 0{\cdot}4$, which for $n = 2$ corresponded to a pure prolate-to-oblate oscillation with a ratio of the major L to minor W axis at maximum deformation of $\alpha \equiv L/W \approx 1{\cdot}81$. This value of ϵ has been chosen so that the correction to the shape at order ϵ^3 will be $O(10^{-2})$ of the deformation (assuming $F^{(3)}(\theta,t) = O(1)$) and so that the shapes in figures 1 and 2 show the same magnitude of deformation as the numerical calculations of Foote (1973) and Alonso (1974).

For the shapes in figure 1, the drop had its largest distortion at $t = 0$ when it had no velocity. The linear theory predicted a perfectly spherical shape after a quarter of the period ($t = \frac{1}{2}\pi$). The second-order corrections deformed this sphere into a prolate shape for the fundamental ($n = 2$) mode of oscillation and into multilobed forms for the $n = 3$ and $n = 4$ modes. At $t = \pi$ the distortion of the shape was again maximum and the velocity zero. For times between π and 2π the drop retraced the shapes in its evolution between $t = 0$ and π.

The differences between the contributions of inertia in drops and bubbles are seen by comparing the second-order approximations shown in figures 1 and 2. Two-, three- and four-lobed drop oscillations were much more elongated along the axis of symmetry for $\frac{1}{4}\pi \leqslant t \leqslant \frac{3}{4}\pi$ than corresponding oscillating bubbles. For $n = 2$ mode oscillation, the coefficient for the term $P_2(\theta)$ in (42) was largest in the second-order correction for the drop shape, whereas the term proportional to $P_4(\theta)$ dominated the correction (57) for the bubble. For the $n = 4$ oscillation mode, the shapes of the drop and bubble became qualitatively different for $\frac{1}{4}\pi \leqslant t \leqslant \frac{3}{4}\pi$. For t near $\frac{1}{2}\pi$, the bubble had an eight-lobed shape, while the drop had a four-lobed form at the same times; compare figures 1(m) and 2(m).

A number of the asymptotic results for oscillating drops can be compared directly with the numerical calculations of Foote (1973) and Alonso (1974) for viscous drops oscillating in the fundamental mode. The effect of viscosity on the frequency of oscillation and on the shape of the drop is small when the product $(\sigma R/\nu^2\rho)^{\frac{1}{2}}$ is large, where ν is the kinematic viscosity (see Chandrasekhar 1961). In the calculations of Foote ($R = 0{\cdot}06$ cm, $\nu = 0{\cdot}06$ cm^2 s^{-1}, $\sigma = 75$ dyn cm^{-1}, $\rho = 1$ g cm^{-3}, $\alpha = 1{\cdot}7$) and Alonso ($R = 0{\cdot}66 \times 10^{-12}$ cm, $\nu = 0{\cdot}75 \times 10^{-4}$ cm^2 s^{-1}, $\sigma = 1{\cdot}60 \times 10^{20}$ dyn cm^{-1}, $\rho = 1{\cdot}66 \times 10^{15}$ g cm^{-3}, $\alpha = 1{\cdot}8$ and $2{\cdot}5$) this ratio was 35·4 and 3·3 respectively. Thus

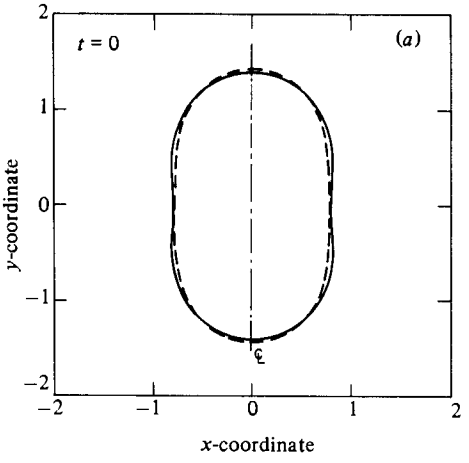

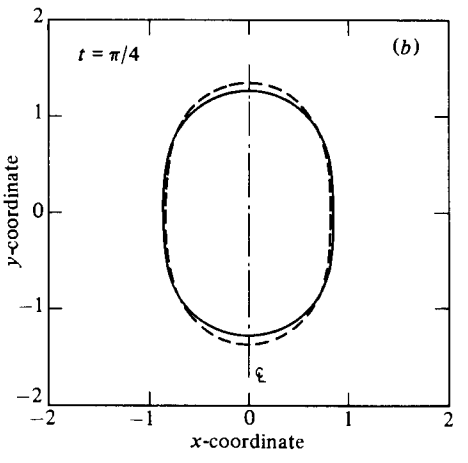

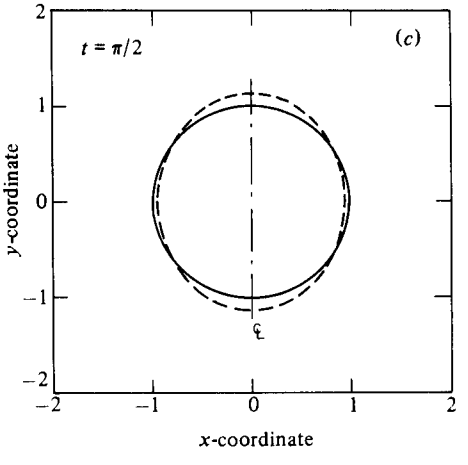

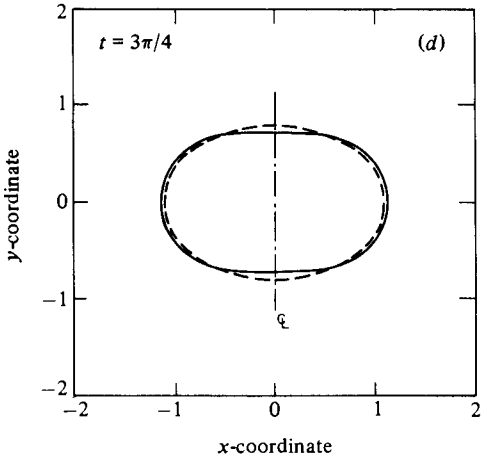

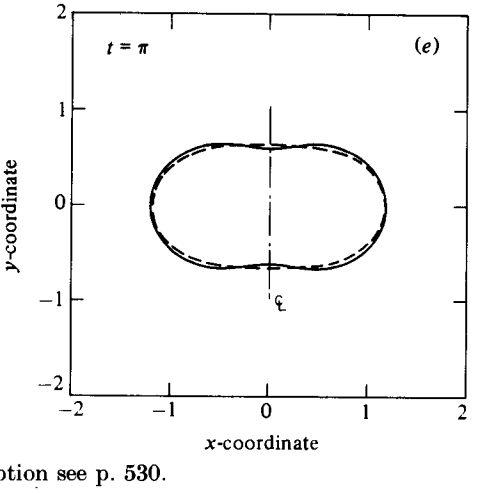

FIGURE 1 (*a–e*). For caption see p. 530.

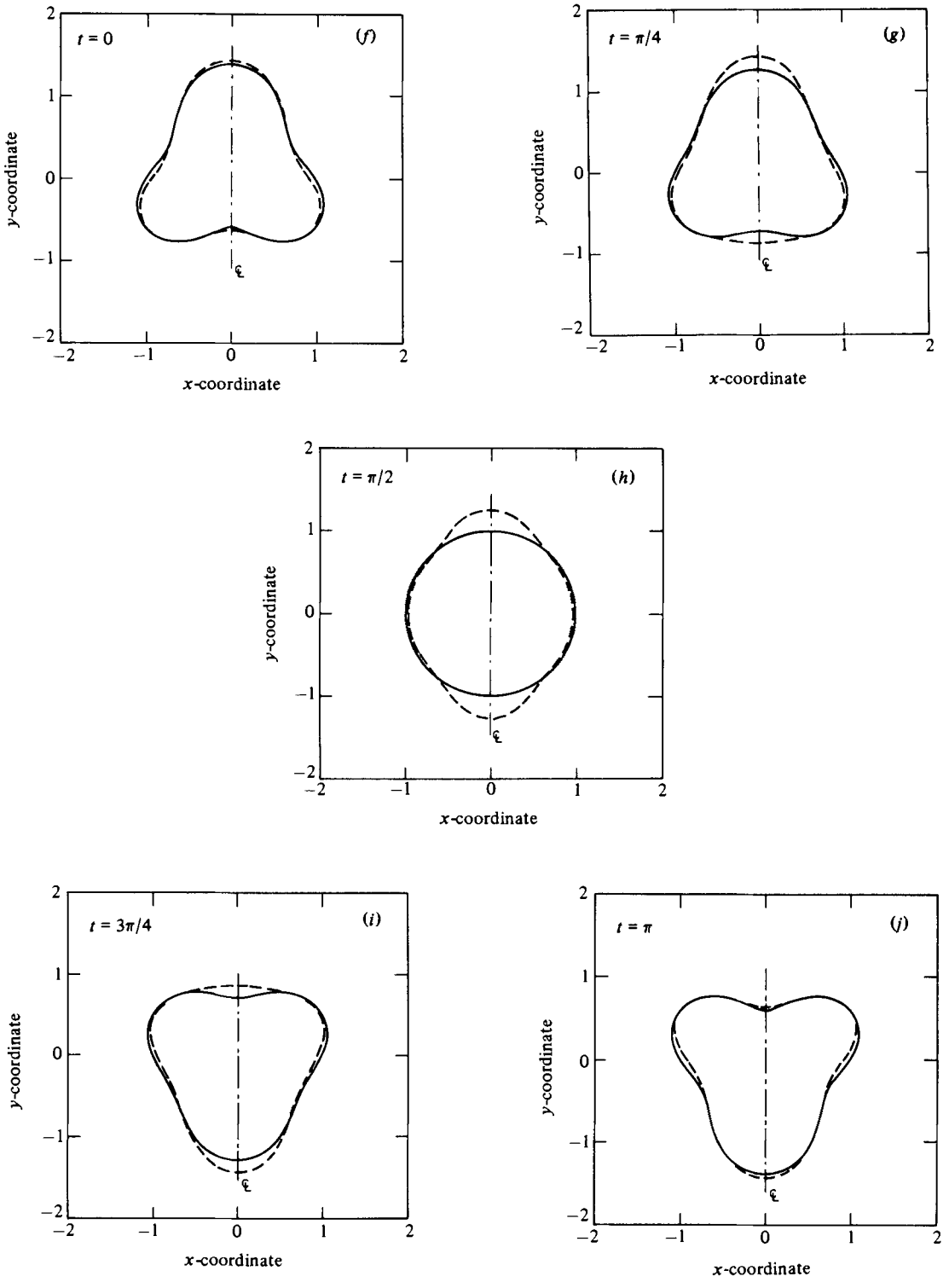

FIGURE 1 (*f–i*). For caption see p. 530.

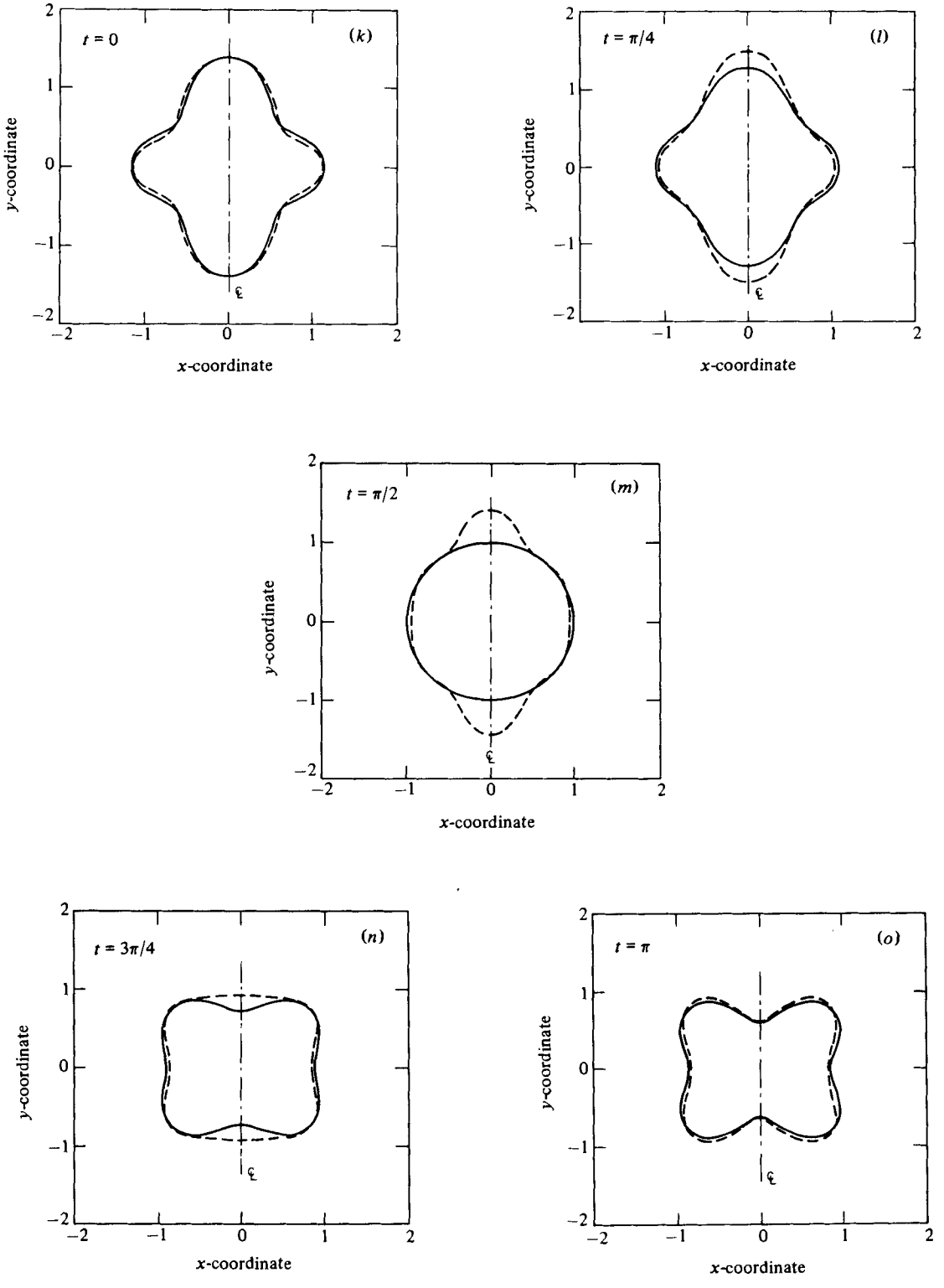

FIGURE 1. Shapes of drops oscillating in the $n = 2$ (*a–e*), $n = 3$ (*f–j*) and $n = 4$ (*k–o*) modes for the amplitude $\epsilon = 0{\cdot}4$. The solid (——) and dashed (– – –) curves are respectively the first- and second-order approximations to the drop shapes.

the comparison of Foote's calculations with our inviscid theory is reasonable, while Alonso's results may deviate substantially solely because of viscosity.

The drop shapes shown in figure 1 are in qualitative agreement with those calculated by Foote and by Alonso. Several other points of agreement are worth mentioning. As noted by Foote, the linear theory predicted shapes that were slightly re-entrant when $t = 0$. This feature was not apparent in either our asymptotic results correct to second order (see figure 1*a*) or in Foote's numerical results. Alonso used least-squares techniques to fit her numerically calculated shapes with a sequence of Legendre polynomials and discovered that the shapes were well represented by sums of the $P_2(\theta)$ and $P_4(\theta)$ functions alone, as predicted by (25) and (42). Also, the sine-squared time dependence of the kinetic and potential energies predicted in equation (52) agreed with the calculations of both Foote and Alonso.

A drop undergoing $n = 2$ oscillations spent a considerably longer part of each period in a prolate form than in an oblate one. The percentage excess time is shown in figure 3 as a function of the amplitude of the oscillation, as measured by $\alpha \equiv L/W$. Also shown in this figure are the results of Foote (1973) that have been extrapolated from the data point ($\alpha = 1{\cdot}7$, excess time = 14 %) and his comment that the excess time varied linearly with oscillation amplitude. The agreement is reasonable. Bubbles exhibited only a slight tendency to stay in prolate forms, as shown by the line on figure 3.

The quadratic decrease in frequency with amplitude predicted here is compared on figure 4 to the numerical results of Foote and Alonso. The asymptotic results are within ten per cent of Foote's viscous calculations over the entire range of amplitude $0 \leqslant \alpha \leqslant 1{\cdot}8$ presented by that author. The single value calculated from Alonso's report differed more significantly from our results.

Finally, the inviscid predictions are compared on figures 3 and 4 to experimental results of Trinh & Wang (1982) for almost neutrally buoyant drops of silicone oil and carbon tetrachloride suspended in distilled water. The shapes were set into oscillation by acoustically driving the drop near its fundamental frequency. The driver was then turned off and the drop motion evolved into free oscillation. In the limits of moderate-amplitude oscillations and large drops ($R \approx 1$ cm), the oscillation frequencies measured this way were expected to be near those of an inviscid liquid/liquid system. This conclusion was reached by calculating the viscous correction to the inviscid frequency derived by Prosperetti (1980, see figure 14) using the physical parameters from the experiments of Trinh & Wang.†

Trinh & Wang's measurements for the percentage of time spent in prolate shapes by the neutrally buoyant drop are shown on figure 3, and, as expected, are bracketed by the inviscid calculations for drops and bubbles. Experimental data for the dependence of frequency on amplitude for drops with radii of 0·62 cm (□) and 0·49 cm (●) are shown on figure 4. The data for the larger drop is again described by an asymptotic result intermediate to the calculations for drops and bubbles for α less than 1·7. The experimental measurements for the smaller drop differ systematically from the inviscid results; this difference may represent the coupling between viscosity and the finite-amplitude motion.

† We have assumed $\sigma = 40$ dyn cm^{-1} as a reasonable interfacial tension for a clean oil/water interface.

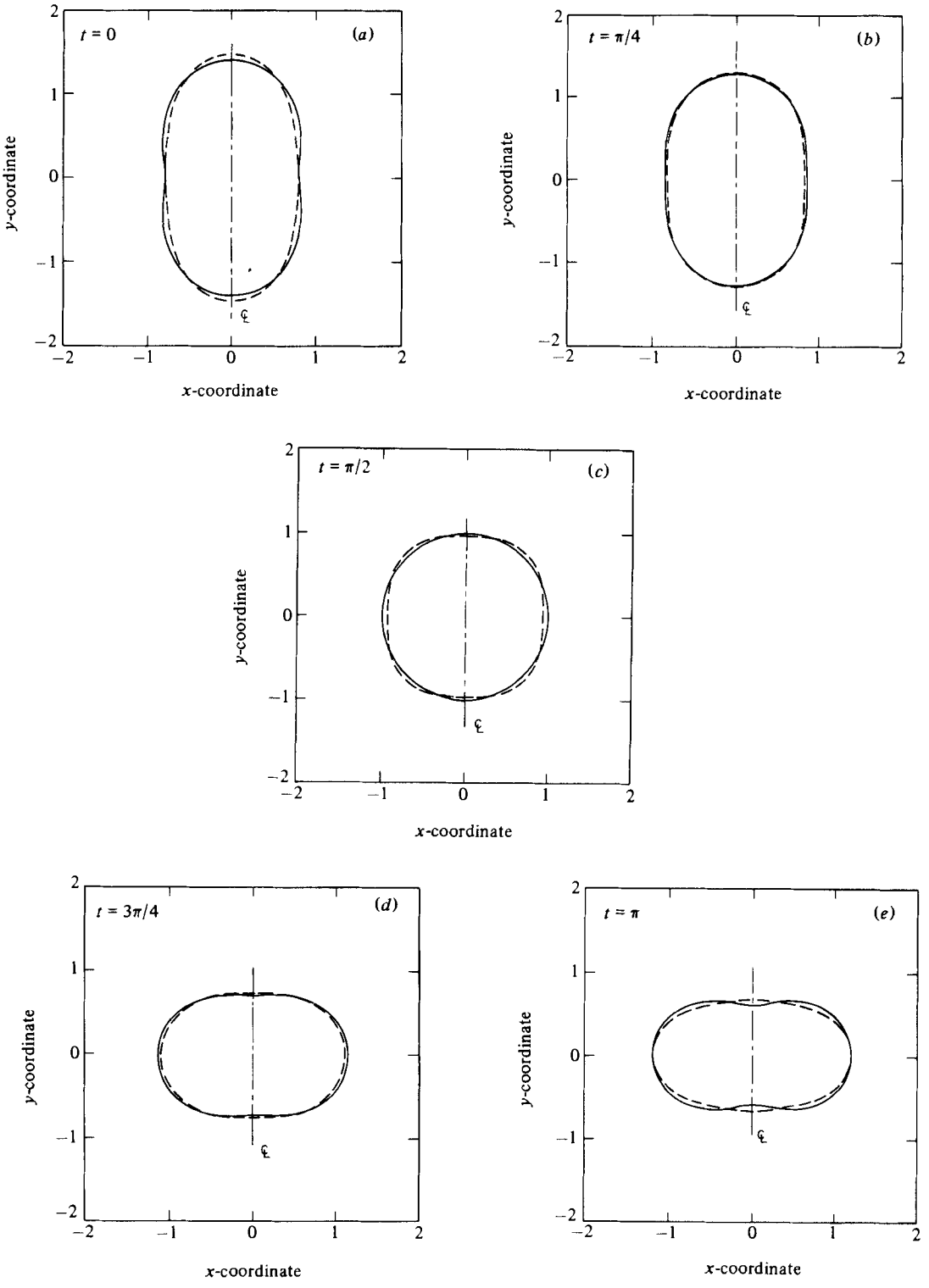

FIGURE 2(*a–e*). For caption see p. 534.

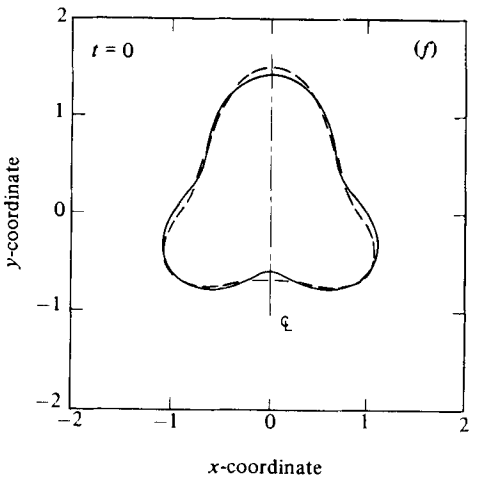

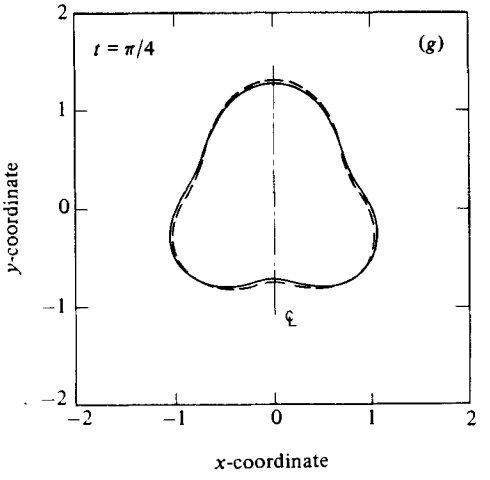

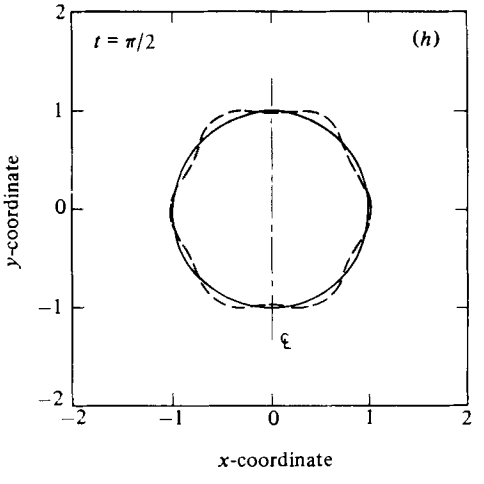

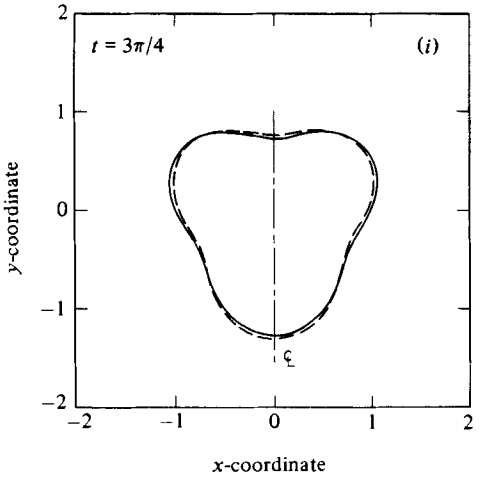

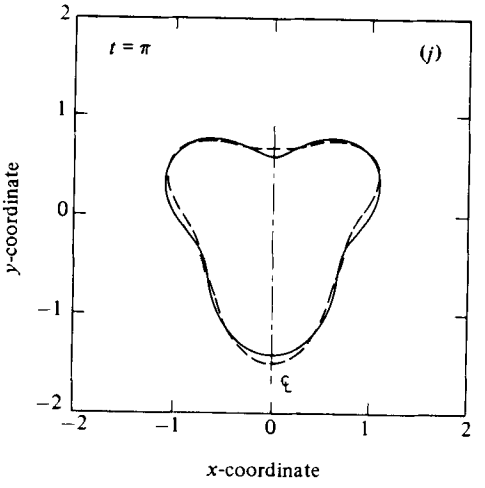

FIGURE 2(*f–j*). For caption see p. 534.

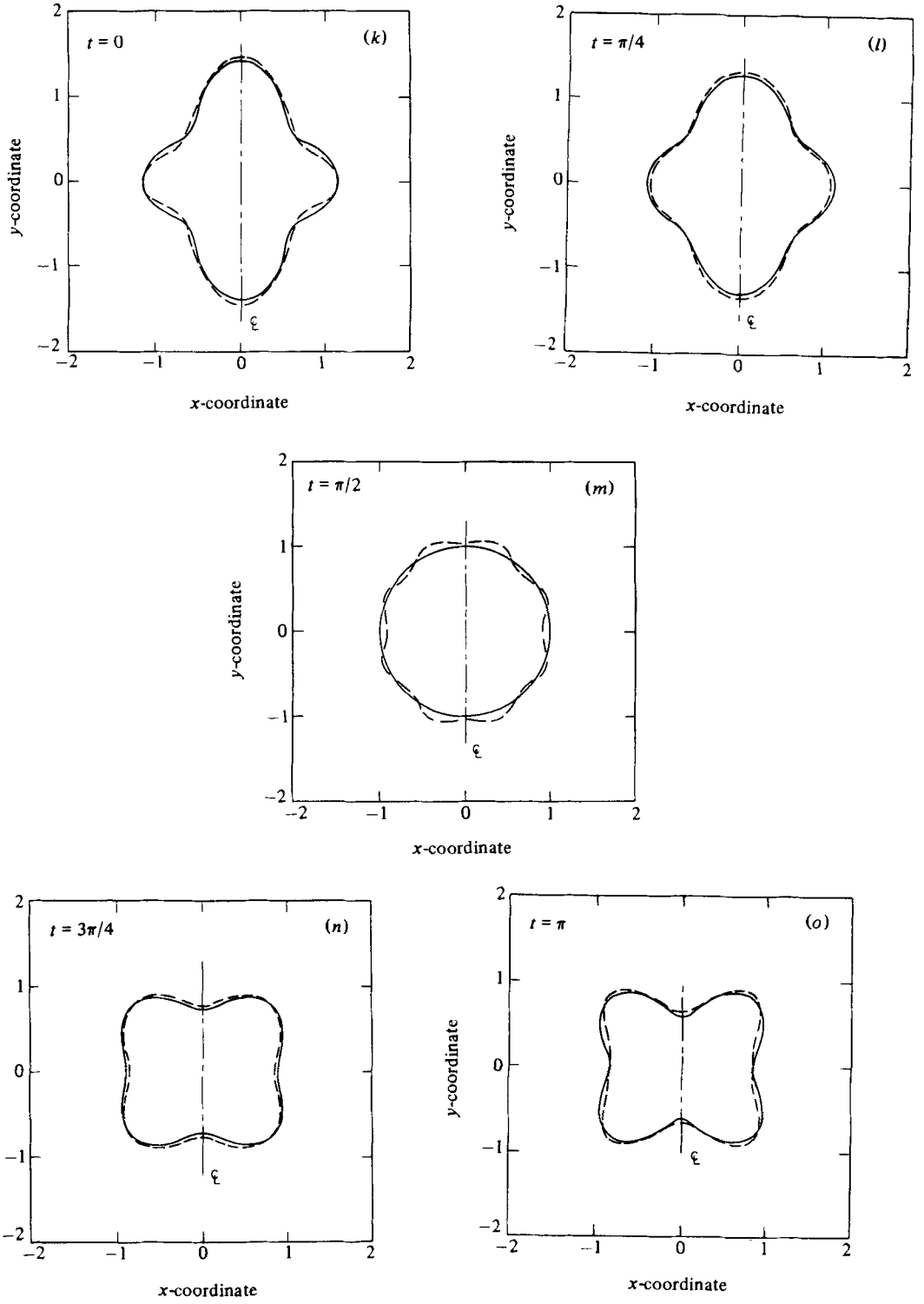

FIGURE 2. Shapes of bubbles oscillating in the $n = 2$ (a–e), $n = 3$ (f–j) and $n = 4$ (k–o) modes for the amplitude $\epsilon = 0{\cdot}4$. The solid (——) and dashed (– – –) curves are respectively the first- and second-order approximations to the drop shapes.

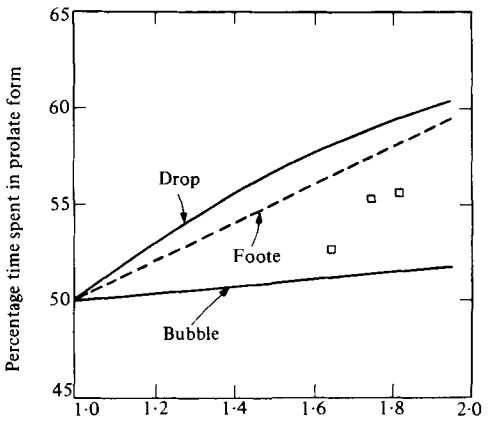

FIGURE 3. The percentage of each period that a drop in $n = 2$ oscillation spends in a prolate shape as a function of the amplitude of the oscillation measured by the maximum ratio of the major to minor axes L/W. Asymptotic results (——), numerical calculations (– – –) of Foote (1973) and experimental results (□) of Trinh & Wang (1980) are shown.

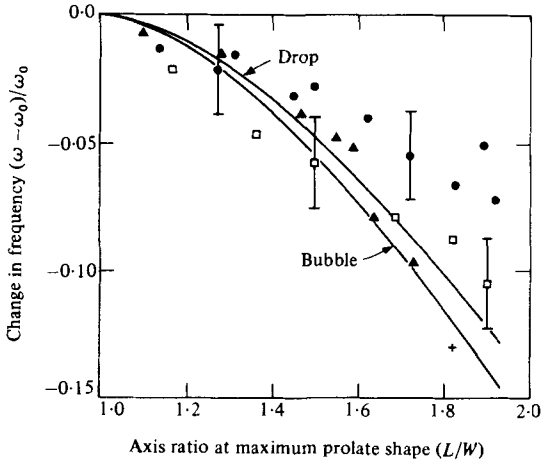

FIGURE 4. The change in $n = 2$ oscillation frequency with increasing amplitude of oscillation as measured by L/W. Asymptotic results (solid curves), numerical calculations of Foote (▲) and Alonso (+), and experimental results of Trinh and Wang (●, $R = 0{\cdot}49$ cm; □, $R = 0{\cdot}62$ cm) are shown.

5. Summary and conclusions

A general theory has been derived for the moderate-amplitude time-periodic oscillations of inviscid drops and bubbles. The variations with amplitude of the drop shape, velocity field and the frequency of oscillation have been calculated in terms of simple expressions. The asymptotic results are in good agreement with numerical calculations for slightly viscous drops. The decrease in frequency caused by increasing the amplitude of motion agrees quantitatively with the numerical calculations of Foote (1973) and is in reasonable agreement with neutrally buoyant experiments for two-liquid systems, considering that the formation of the viscous boundary layer at

the interface and its interaction with the amplitude of the oscillation has been ignored in our comparison.

The stability of the finite-amplitude motions reported here is not mathematically guaranteed and can only be examined by calculating the evolution of small-amplitude perturbations in much the same way as reported by Hall & Seminara (1980) for a bubble undergoing spherosymmetric oscillations. Such an analysis may lead to new insights into the dynamics of the fissioning of drops.

This research was partially supported by a fellowship to J. A. T. from the Department of Chemical Engineering at M.I.T. The authors are also indebted to L. E. Scriven for some timely discussions concerning this work. We also acknowledge the use of MACSYMA at M.I.T.

Appendix

Integrals of products of Legendre polynomials and their derivatives are conveniently written in terms of the $3j$ and $6j$ symbols (Rotenberg *et al.* 1959; Brink & Satchler 1968). Several integrals used in the analysis presented here are

$$I_1 \equiv \int_0^\pi P_n(\theta)\, P_m(\theta)\, P_l(\theta) \sin\theta\, d\theta = 2\begin{pmatrix} n & m & l \\ 0 & 0 & 0 \end{pmatrix}^2, \tag{A 1}$$

$$I_2 \equiv \int_0^\pi P'_n(\theta)\, P'_m(\theta)\, P_l(\theta) \sin\theta\, d\theta = -2[n(n+1)\, m(m+1)]^{\frac{1}{2}} \begin{pmatrix} n & m & l \\ 1 & -1 & 0 \end{pmatrix} \begin{pmatrix} n & m & l \\ 0 & 0 & 0 \end{pmatrix} \tag{A 2}$$

$$I_3 \equiv \int_0^\pi P_n(\theta)\, P_m(\theta)\, P_l(\theta)\, P_k(\theta) \sin\theta\, d\theta = 2 \sum_{j=|n-m|}^{n+m} (2j+1) \begin{pmatrix} n & m & j \\ 0 & 0 & 0 \end{pmatrix}^2 \begin{pmatrix} l & k & j \\ 0 & 0 & 0 \end{pmatrix}^2, \tag{A 3}$$

$$I_4 \equiv \int_0^\pi P'_n(\theta)\, P'_m(\theta)\, P_l(\theta)\, P_k(\theta) \sin\theta\, d\theta = -2[n(n+1)\, m(m+1)]^{\frac{1}{2}} \times \sum_{j=|n-m|}^{n+m} (2j+1) \begin{pmatrix} n & m & j \\ 1 & -1 & 0 \end{pmatrix} \begin{pmatrix} n & m & j \\ 0 & 0 & 0 \end{pmatrix} \begin{pmatrix} l & k & j \\ 0 & 0 & 0 \end{pmatrix}^2. \tag{A 4}$$

Properties of the symbol $\begin{pmatrix} n & m & l \\ a & b & c \end{pmatrix}$ cause it to be zero whenever the triangle inequality ($|l-m| \leqslant n \leqslant l+m$) is not satisfied between the integers of the first row. It is this property that terminates the expansions (e.g. (15) and (34)) for the drop shapes and potentials. This symbol is also identically zero when $a+b+c \neq 0$, or when $a = b = c = 0$ and simultaneously $n+m+l = 2\lambda+1$, where $\lambda = 0, 1, 2, \ldots$. It is this last property that eliminates the odd-order Legendre polynomials from the second-order approximation.

REFERENCES

Alonso, C. T. 1974 The dynamics of colliding and oscillating drops. In *Proc. Int. Colloq. on Drops and Bubbles* (ed. D. J. Collins, M. S. Plesset & M. M. Saffren). Jet Propulsion Laboratory.

Brink, D. M. & Satchler, G. R. 1968 *Angular Momentum*, 2nd ed. Clarendon.

Chandrasekhar, S. 1961 *Hydrodynamic and Hydromagnetic Stability*. Oxford University Press.

Concus, P. 1962 Standing capillary-gravity waves of finite amplitude. *J. Fluid Mech.* **14**, 568–576.

FOOTE, G. B. 1973 A numerical method for studying simple drop behavior: simple oscillation. *J. Comp. Phys.* **11**, 507–530.

HALL, P. & SEMINARA, G. 1980 Nonlinear oscillations of non-spherical cavitation bubbles in acoustic fields. *J. Fluid Mech.* **101**, 423–444.

JOSEPH, D. D. 1973 Domain perturbations: the higher order theory of infinitesimal water waves. *Arch. Rat. Mech. Anal.* **51**, 295–303.

LAMB, H. 1932 *Hydrodynamics*, 6th ed. Cambridge University Press.

MACSYMA 1977 *Reference Manual.* Laboratory of Computer Science, Massachusetts Institute of Technology.

MARSTON, P. L. 1980 Shape oscillation and static deformation of drops and bubbles driven by modulated radiation stresses: theory. *J. Acoust. Soc. Am.* **67**, 15–26.

MARSTON, P. L. & APFEL, R. E. 1979 Acoustically forced shape oscillation of hydrocarbon drops levitated in water. *J. Colloid Interface Sci.* **68**, 280–286.

MARSTON, P. L. & APFEL, R. E. 1980 Quadrapole resonance of drops driven by modulated acoustic radiation pressure: experimental properties. *J. Acoust. Soc. Am.* **67**, 27–37.

MILLER, C. A. & SCRIVEN, L. E. 1968 The oscillations of a fluid droplet immersed in another fluid. *J. Fluid Mech.* **32**, 417–435.

NAYFEH, A. H. & MOOK, D. T. 1979 *Nonlinear Oscillations.* Wiley-Interscience.

PAVELLE, R., ROTHSTEIN, M. & FITCH, J. 1981 Computer algebra. *Sci. Am.* **245**, 136–152.

PLATEAU, J. A. F. 1873 *Statique Expérimentale et Théorique des liquides soumis aux seules forces moléculaires.* Gauthier-Villars.

PROSPERETTI, A. 1980 Normal-mode analysis for the oscillations of a viscous liquid drop in an immiscible liquid. *J. Méc.* **19**, 149–182.

RAYLEIGH, J. W. S. 1879 On the capillary phenomena of jets. *Proc. R. Soc. Lond.* **29**, 71–97.

REID, W. H. 1960 The oscillations of a viscous liquid drop. *Q. Appl. Math.* **18**, 86–89.

ROTENBERG, M., BIVINS, R., METROPOLIS, N. & WOOTEN, J. K. 1959 *The 3j and 6j Symbols.* Technology Press.

SAVART, F. 1833 Mémoire sur la constitution des veines liquides lancées par des orifices circulaires en mince paroi. *Ann. de Chim.* **53**, 337–386.

TADJBAKHSH, I. & KELLER, J. B. 1960 Standing surface waves of finite amplitude. *J. Fluid Mech.* **8**, 442–451.

TRINH, E., ZWERN, A. & WANG, T. G. 1982 An experimental study of small-amplitude drop oscillations in immiscible liquid systems. *J. Fluid Mech.* **115**, 453–474.

TRINH, E. & WANG, T. G. 1982 Large amplitude drop shape oscillations. In *Proc. 2nd Int. Colloq. on Drops and Bubbles. JPL Publ.* 82–87, *Pasadena.*

TSAMOPOULOS, J. A. 1983 Ph.D. thesis, Massachusetts Institute of Technology (in preparation).